Extending Wang's 1D Sn Analytic Solution to Heterogeneous Problems with No Iteration on Interfacial Fluxes

Zeyun Wu

Department of Mechanical and Nuclear Engineering, Virginia Commonwealth University,
401 West Main Street, Richmond, VA 23284, zwu@vcu.edu
https://dx.doi.org/10.13182/T30953

INTRODUCTION

Analytic techniques for one-dimensional (1D) transport problems can produce extremely accurate benchmark solutions with no spatial errors, which provide an efficient means to verify new proposed numerical spatial discretization approaches for transport method development. Furthermore, highly accurate 1D solutions can benefit the development of nodal transport methods which use the transverse integration approach to convert the multi-dimensional transport equation to a set of coupled 1D ones [1]. Partly due to these reasons, the decades old problem, obtaining an analytic solution for the 1D monoenergetic Sn neutron transport equation in slab geometry, has been frequently visited by many researchers over the last few decades [1-5]. Most recently, Wang et al. proposed one solution to this problem based on some novel features from all the former approaches [6]. Wang's approach employs an eigen-decomposition procedure of the transport-scattering operator in the Sn equation and takes advantage of the eigenvalues and eigenvectors yielded from the decomposition to generate the analytic solutions. This idea may bear some similarities to some former work [7, 8], and has the same essence as the analytic approach recently proposed by English and Wu [9]. The techniques used in these approaches to construct the flux solution are somehow all different. In Wang's method [6], a closed form of the analytic solution is established in a neat expression that only has matrix-vector multiplications. This closed form provides substantial convenience and flexibility to generate analytic solution at any position of the problem. Moreover, numerical experiment shows it possesses superior efficiency by computing the solution with the closed form without invoking any intermediate processes. A brief review of Wang's 1D analytic solution is presented in the next section.

However, some application limitations were observed in Wang's analytic solution presented in Ref. 6. For example, the solution only considers vacuum boundaries or arbitrary incident flux boundaries – the solution may require changes for reflective boundaries. Extension to high order of anisotropic scattering appears to be straightforward, whereas the original form is limited to the isotropic scattering cases only. Problems with void regions are excluded for ease of implementation. Moreover, the presentation is only focused on a one-region homogeneous problem. Although numerical experiments demonstrate the results for a multi-region problem, it was achieved through an iteration procedure.

To remove these limitations and to fully realize the benefits of the closed form of the 1D analytic solution, this paper presents some recent efforts that substantially extend the applications of Wang's 1D analytic solution to the Sn transport problem. These efforts make the new solution applicable to various conditions including heterogeneous situation, variety of boundary conditions, arbitrary order of scattering anisotropy, and void regions. In particular, the extended solution has removed the iteration procedure needed for heterogeneous problems, and replaced it with a direct method that solves a system of linear equations. Numerical results are provided at the end of the summary to verify the method implementations.

WANG'S 1D SN ANALYTIC SOLUTION

With standard notations, the monoenergetic Sn transport equation in slab geometry with homogeneous media and constant external neutron source is written as

$$\begin{aligned}&\mu_m \frac{d\psi_m(x)}{dx} + \Sigma_t(x)\psi_m(x) \\ &= \sum_{l=0}^{L} \frac{2l+1}{2} \Sigma_{sl}(x) P_l(\mu_m)\phi_l(x) + \frac{Q}{2},\ m = 1,\cdots,N.\end{aligned} \tag{1}$$

where N is the order of quadrature set the Sn method. Standard Gaussian Legendre quadrature set was used in this work. L is the order of scattering anisotropy approximated for the angular differential scattering cross section, and $\phi_l(x)$ is the angular flux moment defined as

$$\phi_l(x) = \sum_{m'=1}^{N} w_{m'} P_l(\mu_{m'})\psi_{m'}(x) \ . \tag{2}$$

Eq. may be written into a matrix-vector form

$$\frac{d\boldsymbol{\psi}(x)}{dx} + \mathbf{A}\boldsymbol{\psi}(x) = \mathbf{b}\ , \tag{3}$$

where the vector terms ($\boldsymbol{\psi}$ and $\mathbf{b}$) and the full matrix $\mathbf{A}$ are

$$\boldsymbol{\psi}(x) = \begin{bmatrix}\psi_1(x)\\ \psi_2(x)\\ \vdots\\ \psi_N(x)\end{bmatrix}, \qquad \mathbf{b} = \frac{Q}{2}\begin{bmatrix}1/\mu_1\\ 1/\mu_2\\ \vdots\\ 1/\mu_N\end{bmatrix}\ , \tag{4}$$

$$\mathbf{A}=\begin{bmatrix} \frac{1}{\mu_1}\left(\Sigma_t-\sum_{l=0}^{L}\frac{2l+1}{2}\Sigma_{sl}P_l(\mu_1)w_1P_l(\mu_1)\right) & -\frac{1}{\mu_1}\left(\sum_{l=0}^{L}\frac{2l+1}{2}\Sigma_{sl}P_l(\mu_1)w_2P_l(\mu_2)\right) & \cdots & -\frac{1}{\mu_1}\left(\sum_{l=0}^{L}\frac{2l+1}{2}\Sigma_{sl}P_l(\mu_1)w_NP_l(\mu_N)\right) \\ -\frac{1}{\mu_2}\left(\sum_{l=0}^{L}\frac{2l+1}{2}\Sigma_{sl}P_l(\mu_2)w_1P_l(\mu_1)\right) & \frac{1}{\mu_2}\left(\Sigma_t-\sum_{l=0}^{L}\frac{2l+1}{2}\Sigma_{sl}P_l(\mu_2)w_2P_l(\mu_2)\right) & \vdots & -\frac{1}{\mu_2}\left(\sum_{l=0}^{L}\frac{2l+1}{2}\Sigma_{sl}P_l(\mu_2)w_NP_l(\mu_N)\right) \\ \vdots & \vdots & \ddots & \vdots \\ -\frac{1}{\mu_N}\left(\sum_{l=0}^{L}\frac{2l+1}{2}\Sigma_{sl}P_l(\mu_N)w_1P_l(\mu_1)\right) & -\frac{1}{\mu_N}\sum_{l=0}^{L}\frac{2l+1}{2}\Sigma_{sl}P_l(\mu_N)w_2P_l(\mu_2) & \cdots & \frac{1}{\mu_N}\left(\Sigma_t-\sum_{l=0}^{L}\frac{2l+1}{2}\Sigma_{sl}P_l(\mu_N)w_NP_l(\mu_N)\right) \end{bmatrix}. \quad (5)$$

Note the constant source, Q, is incorporated into the vector **b** for simplicity and the matrix **A** has a size of $N \times N$.

For a slab with a size of X cm, the left and right boundary conditions (if non-reflective) can be generally described as follows, respectively

$$\begin{aligned} \psi_m^L &= \psi_m(0) = f_m, \quad \text{for } \mu_m > 0, \\ \psi_m^R &= \psi_m(X) = g_m, \quad \text{for } \mu_m < 0. \end{aligned} \quad (6)$$

Here F_M and g_m are prescribed incident fluxes on the outer boundaries. For illustration, the configuration of the problem with known boundary conditions is depicted in Fig. 1. The meaning of the vectors shown in the figure is obvious. For example, the boundary conditions given in Eq.(6) are compactly represented by vector $\boldsymbol{\psi}_L^+$ and $\boldsymbol{\psi}_R^-$.

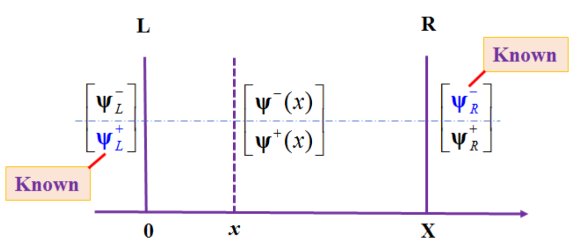

Figure 1. Configuration of a 1D homogeneous slab.

In general, the matrix **A** in Eq.(3) is diagonalizable and thus can be decomposed with the standard eigen-decomposition procedure

$$\mathbf{A} = \mathbf{R}\boldsymbol{\Lambda}\mathbf{R}^{-1}, \quad (7)$$

where $\boldsymbol{\Lambda}$ is a diagonal matrix with diagonal elements corresponding to eigenvalues of **A**, **R** is a matrix with column vectors corresponding to the eigenvectors of **A**. With this decomposition, we re-write Eq.(3) as

$$\frac{d\boldsymbol{\psi}(x)}{dx} + \mathbf{R}\boldsymbol{\Lambda}\mathbf{R}^{-1}\boldsymbol{\psi}(x) = \mathbf{b}\,. \quad (8)$$

If we define a *pseudo-angular flux* vector

$$\boldsymbol{\varphi} = \mathbf{R}^{-1}\boldsymbol{\psi}\,, \quad (9)$$

we can rewrite Eq.(8) as

$$\frac{\partial \boldsymbol{\varphi}(x)}{\partial x} + \boldsymbol{\Lambda}\boldsymbol{\varphi}(x) = \mathbf{R}^{-1}\mathbf{b}\,. \quad (10)$$

Because $\boldsymbol{\Lambda}$ is a diagonal matrix, we can easily obtain the analytic solution of Eq.(10), which is essentially a system of ODEs. This solution can then be reverted back to the desired flux solution using Eq. (9). This is how the closed form of Wang's analytic solution obtained. The procedure involves a little bit algebraic arrangement, but the final solution is a very clean one shown as follows

$$\begin{aligned} \begin{bmatrix} \boldsymbol{\psi}^-(x) \\ \boldsymbol{\psi}^+(x) \end{bmatrix} &= \mathbf{R}\begin{bmatrix} e^{\boldsymbol{\Lambda}^-(X-x)} & \\ & e^{-\boldsymbol{\Lambda}^+x} \end{bmatrix}\begin{bmatrix} \boldsymbol{\varphi}_R^- \\ \boldsymbol{\varphi}_L^+ \end{bmatrix} \\ &+ \frac{Q}{2(\Sigma_t - \Sigma_{s0})}\left(\mathbf{I} - \mathbf{R}\begin{bmatrix} e^{\boldsymbol{\Lambda}^-(X-x)} & \\ & e^{-\boldsymbol{\Lambda}^+x} \end{bmatrix}\mathbf{R}^{-1}\right)\mathbf{1} \end{aligned}, \quad (11)$$

where $\mathbf{I}$ is the identity matrix and $\mathbf{1}$ is a vector with all elements be one, the minus and plus superscript in angular fluxes stand for fluxes with positive and negative ordinates in the Sn equation. $\boldsymbol{\Lambda}^-$ and $\boldsymbol{\Lambda}^+$ are diagonal matrices with corresponding negative and positive eigenvalues. The undetermined vector $\begin{bmatrix} \boldsymbol{\varphi}_R^- & \boldsymbol{\varphi}_L^+ \end{bmatrix}^T$ appearing in the solution are the formal boundary values of the pseudo-fluxes. This vector, which can be determined by physical boundary conditions, makes the closed form solution interesting because it is the only unknown in the solution and the two elements contained in the vector (i.e., $\boldsymbol{\varphi}_R^-$ and $\boldsymbol{\varphi}_L^+$) appears at different physical location of the problem (see Fig.1). This feature of the solution is later shown to provide great advantages on extending the solution to heterogeneous problems, as narrated in the next section.

EXTENSIONS ON THE ANALYTIC SOLUTION

A straightforward way to extend the analytic solution to a multi-region heterogeneous problem is to use the iterative method on the interfacial angular fluxes as they can be treated as incoming flux boundaries for the intermediate regions. The formula given in Eq. (11) can be used to solve the flux distribution in a region-by-region fashion. This iterative approach will become inefficient, particularly when the scattering ratios of some regions become large.

Here we present an alternative yet more efficient approach to handle the heterogeneous case without iterations on the interfacial fluxes. This approach takes advantage of the closed form solution and pre-calculates the sole unknowns (i.e., the vector $\left[\boldsymbol{\varphi}_R^- \quad \boldsymbol{\varphi}_L^+\right]^T$) appeared in the solution for each region. Along the procedure, the variety of boundary conditions and void regions can be incorporated naturally. For illustration, a two-region problem is shown in Fig. 2, where the unknown (i.e., the pseudo-flux vector) for each region is indicated with red color.

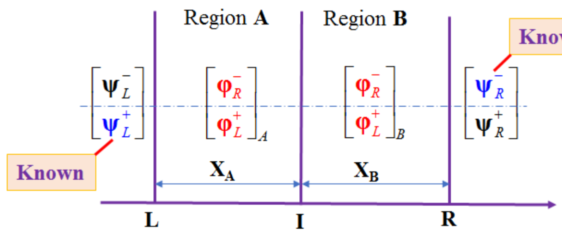

Figure 2. Configuration for a two-region problem in slab.

If separating each unknown vector into two parts, one can see there are really four unknowns in the two-region problem. Without loss of generality, we denote the four unknowns in an order as follows

$$\begin{bmatrix}\boldsymbol{\varphi}_R^- \\ \boldsymbol{\varphi}_L^+\end{bmatrix}_A = \begin{bmatrix}\boldsymbol{\varphi}_1 \\ \boldsymbol{\varphi}_2\end{bmatrix}, \quad \begin{bmatrix}\boldsymbol{\varphi}_R^- \\ \boldsymbol{\varphi}_L^+\end{bmatrix}_B = \begin{bmatrix}\boldsymbol{\varphi}_3 \\ \boldsymbol{\varphi}_4\end{bmatrix}.$$

By defining a source vector

$$\mathbf{q} = \begin{bmatrix}\mathbf{q}^- \\ \mathbf{q}^+\end{bmatrix} = \frac{Q}{2(\Sigma_t - \Sigma_{s0})}\mathbf{R}^{-1}\mathbf{1}, \tag{12}$$

the analytic solution expressed in Eq.(11) may be written into the following two equations

$$\begin{aligned}\boldsymbol{\psi}^-(x) &= \mathbf{R}_{11}e^{\boldsymbol{\Lambda}^-(X-x)}\left(\boldsymbol{\varphi}_R^- - \mathbf{q}^-\right) \\ &+\mathbf{R}_{12}e^{-\boldsymbol{\Lambda}^+x}\left(\boldsymbol{\varphi}_L^+ - \mathbf{q}^+\right) + \frac{Q}{2(\Sigma_t - \Sigma_{s0})}\mathbf{1}\end{aligned}, \tag{13}$$

and

$$\begin{aligned}\boldsymbol{\psi}^+(x) &= \mathbf{R}_{21}e^{\boldsymbol{\Lambda}^-(X-x)}\left(\boldsymbol{\varphi}_R^- - \mathbf{q}^-\right) \\ &+\mathbf{R}_{22}e^{-\boldsymbol{\Lambda}^+x}\left(\boldsymbol{\varphi}_L^+ - \mathbf{q}^+\right) + \frac{Q}{2(\Sigma_t - \Sigma_{s0})}\mathbf{1}\end{aligned}. \tag{14}$$

where $\mathbf{R}_{11}$, $\mathbf{R}_{12}$, $\mathbf{R}_{21}$, and $\mathbf{R}_{22}$ are sub-matrices in $\mathbf{R}$.

At the left boundary (x = L in Fig. 2), if the incoming flux ($\boldsymbol{\psi}_L^+$) is known, we set x = 0 in Eq.(14) and get

$$\begin{aligned}&\left(\mathbf{R}_{21}e^{\boldsymbol{\Lambda}^-X}\right)_A\boldsymbol{\varphi}_1 + \left(\mathbf{R}_{22}\right)_A\boldsymbol{\varphi}_2 \\ &= \left(\mathbf{R}_{21}e^{\boldsymbol{\Lambda}^-X}\mathbf{q}^- + \mathbf{R}_{22}\mathbf{q}^+ - \frac{Q}{2(\Sigma_t - \Sigma_{s0})}\mathbf{1}\right)_A + \boldsymbol{\psi}_L^+\end{aligned}. \tag{15}$$

However, if the left boundary is reflective, we get

$$\begin{aligned}&\left[\left(\mathbf{R}_{21} - \mathbf{T}\mathbf{R}_{11}\right)e^{\boldsymbol{\Lambda}^-X}\right]_A\boldsymbol{\varphi}_1 + \left(\mathbf{R}_{22} - \mathbf{T}\mathbf{R}_{12}\right)_A\boldsymbol{\varphi}_2 \\ &= \begin{bmatrix}\left(\mathbf{R}_{21} - \mathbf{T}\mathbf{R}_{11}\right)e^{\boldsymbol{\Lambda}^-X}\mathbf{q}^- + \left(\mathbf{R}_{22} - \mathbf{T}\mathbf{R}_{12}\right)\mathbf{q}^+ \\ +\dfrac{Q}{2(\Sigma_t - \Sigma_{s0})}\left(\mathbf{T} - \mathbf{I}\right)\mathbf{1}\end{bmatrix}_A\end{aligned}, \tag{16}$$

where $\mathbf{T}$ is a mirror reflective matrix that connects the positive and negative portion of the angular flux at the boundary

$$\boldsymbol{\psi}_L^- = \mathbf{T}\boldsymbol{\psi}_L^+ . \tag{17}$$

The equations at the right boundary (x = R in Fig. 2) can be developed similarly. The resulting equations are outlined in Eq.(18) for a known incident boundary and Eq.(19) for a reflective one:

$$\begin{aligned}&\left(\mathbf{R}_{11}\right)_B\boldsymbol{\varphi}_3 + \left(\mathbf{R}_{12}e^{-\boldsymbol{\Lambda}^+X}\right)_B\boldsymbol{\varphi}_4 \\ &= \left(\mathbf{R}_{11}\mathbf{q}^- + \mathbf{R}_{12}e^{-\boldsymbol{\Lambda}^+X}\mathbf{q}^+ - \frac{Q}{2(\Sigma_t - \Sigma_{s0})}\mathbf{1}\right)_B + \boldsymbol{\psi}_R^-\end{aligned} \tag{18}$$

$$\begin{aligned}&\left(\mathbf{R}_{11} - \mathbf{T}\mathbf{R}_{21}\right)_B\boldsymbol{\varphi}_3 + \left[\left(\mathbf{R}_{12} - \mathbf{T}\mathbf{R}_{22}\right)e^{-\boldsymbol{\Lambda}^+X}\right]_B\boldsymbol{\varphi}_4 \\ &= \begin{bmatrix}\left(\mathbf{R}_{11} - \mathbf{T}\mathbf{R}_{21}\right)\mathbf{q}^- + \left(\mathbf{R}_{12} - \mathbf{T}\mathbf{R}_{22}\right)e^{-\boldsymbol{\Lambda}^+X}\mathbf{q}^+ \\ +\dfrac{Q}{2(\Sigma_t - \Sigma_{s0})}\left(\mathbf{T} - \mathbf{I}\right)\mathbf{1}\end{bmatrix}_B\end{aligned} \tag{19}$$

At the interface of the problem (x = I in Fig. 2), if we set x = X_A to the analytic solution at Region A, and x = 0 to the analytic solution at Region B, we obtain the two sets of angular flux solution at the interface. Using the flux continuity condition at the interface, we obtain

$$\begin{aligned}&\left(\mathbf{R}_{11}\right)_A\boldsymbol{\varphi}_1 + \left(\mathbf{R}_{12}e^{-\boldsymbol{\Lambda}^+X}\right)_A\boldsymbol{\varphi}_2 - \left(\mathbf{R}_{11}e^{\boldsymbol{\Lambda}^-X}\right)_B\boldsymbol{\varphi}_3 - \left(\mathbf{R}_{12}\right)_B\boldsymbol{\varphi}_4 \\ &= \left(\mathbf{R}_{11}\mathbf{q}^- + \mathbf{R}_{12}e^{-\boldsymbol{\Lambda}^+X}\mathbf{q}^+ - \frac{Q}{2(\Sigma_t - \Sigma_{s0})}\mathbf{1}\right)_A \\ &- \left(\mathbf{R}_{11}e^{\boldsymbol{\Lambda}^-X}\mathbf{q}^- + \mathbf{R}_{12}\mathbf{q}^+ - \frac{Q}{2(\Sigma_t - \Sigma_{s0})}\mathbf{1}\right)_B\end{aligned}, \tag{20}$$

and

$$\begin{aligned}&\left(\mathbf{R}_{21}\right)_A\boldsymbol{\varphi}_1 + \left(\mathbf{R}_{22}e^{-\boldsymbol{\Lambda}^+X}\right)_A\boldsymbol{\varphi}_2 - \left(\mathbf{R}_{21}e^{\boldsymbol{\Lambda}^-X}\right)_B\boldsymbol{\varphi}_3 - \left(\mathbf{R}_{22}\right)_B\boldsymbol{\varphi}_4 \\ &= \left(\mathbf{R}_{21}\mathbf{q}^- + \mathbf{R}_{22}e^{-\boldsymbol{\Lambda}^+X}\mathbf{q}^+ - \frac{Q}{2(\Sigma_t - \Sigma_{s0})}\mathbf{1}\right)_A \\ &- \left(\mathbf{R}_{21}e^{\boldsymbol{\Lambda}^-X}\mathbf{q}^- + \mathbf{R}_{22}\mathbf{q}^+ - \frac{Q}{2(\Sigma_t - \Sigma_{s0})}\mathbf{1}\right)_B\end{aligned}. \tag{21}$$

Eq.(15) [or Eq.(16) for a reflective boundary], Eq.(20), Eq.(21), and Eq.(18) [or Eq.(19) for a reflective boundary] establish a system of linear equations with block-wise matrices as coefficients. The size of these block matrices or vectors is the half size of the quadrature set (i.e. $N/2$). We can solve for the four unknowns $\{\boldsymbol{\varphi}_1, \boldsymbol{\varphi}_2, \boldsymbol{\varphi}_3, \boldsymbol{\varphi}_4\}$ simultaneously with these equations. If the problem has more intermediate regions, then the pair of equations similar to Eq.(20) and (21) will be repeated to incorporate more unknown vectors into the system of equations. Once these unknown vectors are resolved in each region, we can insert them to the analytic solution given in Eq.(11) to yield angular flux of any arbitrary position in any region.

For a void region, the analytic solution is essentially reduced to the following form

$$\begin{bmatrix} \boldsymbol{\psi}^-(x) \\ \boldsymbol{\psi}^+(x) \end{bmatrix} = \mathbf{R} \begin{bmatrix} \boldsymbol{\varphi}_R^- \\ \boldsymbol{\varphi}_L^+ \end{bmatrix}, \tag{22}$$

where the eigenvector matrix $\mathbf{R}$ is really degraded to an identity matrix, which indicates the flux stays unchanged and the pseudo-flux becomes identical to the real flux.

NUMERICAL RESULTS

We first test the Reed's problem [10] to demonstrate the viability of the proposed approach. The Reed's problem is a 1D heterogeneous source problem that consists of 5 regions. One region (Region 3) is void. The first and second region contains pure absorbers. The constant sources were distributed in Region 1 and 3. The problem was imposed with the reflective boundary condition on the left side and vacuum boundary condition on the right side. More detailed configuration and flux solution of Reed's problem is shown in Fig. 3. Here our solution was compared against the analytic solution provided by Warsa [4] and the agreement is up to the machine error (e.g., 1E-14) between the two solutions, which indicates the high accuracy of the solution produced by our approach.

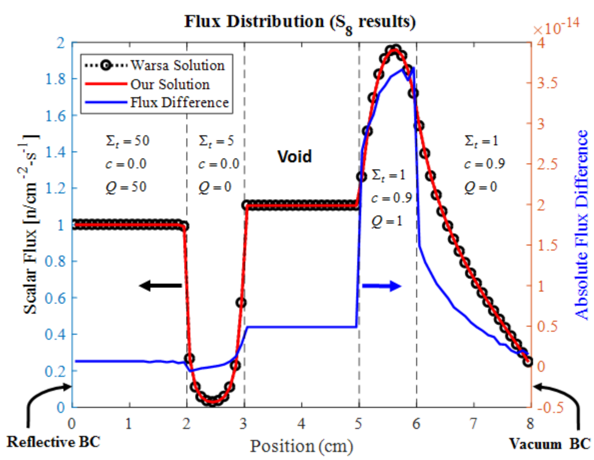

Figure 3. The solution of the Reed's problem.

The second model problem tested is the so-called Iron-Water problem originally proposed by Larsen [11]. It is a four-region heterogeneous problem consisting of diffusive materials with linear scattering anisotropy. The configuration of the problem and the flux solution of our approach comparing to a corrected Warsa's solution [12] is shown in Fig. 4. As can be seen, the absolute deviation of the point-wise flux from the two codes remains in a level of 1E-10. The level of agreement degrades in this problem mainly due to the reduced accuracy of eigenvalues and eigenvectors calculated in our Matlab code owing to the highly scattering materials. A high precision eigen-decomposition will improve the solution.

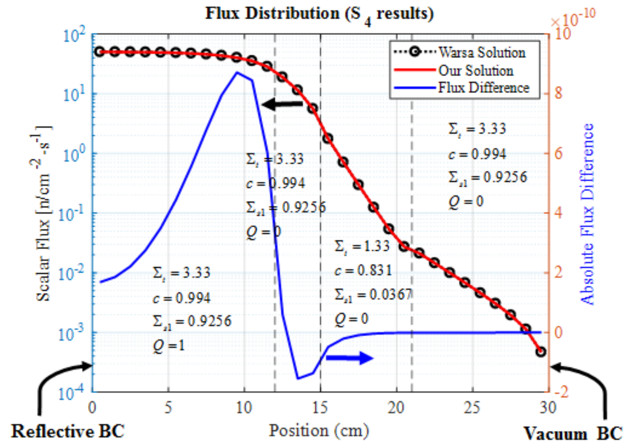

Figure 4. The solution of the Iron-Water problem.

ACKNOWLEDGEMENT

We thank Dean Wang for fruitful discussions on the subject during the writing of the summary.

REFERENCES

1. R. BARROS and E. D. LARSEN, *Nucl. Sci. Eng.* **104**, 199 (1990).
2. C. E. SIEWERT and P. F. ZWEIFEL, *Trans. Am. Nucl. Soc.*, **8**, 504 (1965)
3. M. YAVUZ, *Ann. Nucl. Energy*, **22**, 203 (1995).
4. J. S. WARSA, *Ann. Nucl. Energy*, **29**, 851 (2002).
5. B. D. GANAPOL, *J. Quant. Spectrosc. Radiat. Transfer*, **154**, 72 (2015).
6. D. WANG and T. BYAMBAAKHUU, *Trans. Am. Nucl. Soc.*, **117** (2017).
7. I. P. GRANT and G. E. HUNT, *Proc. Royal Soc. Lond.*, **313**, 183 (1969).
8. P. C. WATERMAN, *J. Opt. Sci. Am.*, **71**, 410 (1981).
9. A. ENGLISH and Z. WU, *PHYTRA-4*, Marrakech, Morocco, September 17-19 (2018).
10. W.H. REED, *Nucl. Sci. Eng.* **46**, 309 (1971).
11. E. W. LARSEN, *Nucl. Sci. Eng.* **83**, 90 (1983).
12. Personal communication.